Observation of Self-Organized Criticality Near the Superfluid Transition in ^{4}He

W. A. Moeur,[1] P. K. Day,[2] F-C. Liu,[2] S. T. P. Boyd,[1] M. J. Adriaans,[3] and R. V. Duncan[1]
[1]*Department of Physics and Astronomy, University of New Mexico, Albuquerque, New Mexico 87131-1156*
[2]*Jet Propulsion Laboratory, MS79-24, Pasadena, California 91109-8099*
[3]*Sandia National Laboratories, MS0980, Albuquerque, New Mexico 87185-0980*
(Received 9 January 1997)

We report on an experimental observation of self-organized criticality in ^{4}He very close to its superfluid transition. A constant temperature gradient, independent of the heat flux Q through the sample, is created along a vertical column of ^{4}He by applying heat to the top of the column. This constant temperature gradient equals the gravity-induced gradient in the superfluid transition temperature, indicating that the thermal conductivity of the sample has self-organized. The closeness to criticality in this state is the same throughout most of the sample, and it depends only on Q. [S0031-9007(97)02801-9]

PACS numbers: 67.40.Kh, 64.60.Ht, 64.60.Lx

In this Letter we report on an observation of self-organized criticality (SOC) in the thermal conductivity κ of ^{4}He near its superfluid transition. Self-organization has been observed in several other physical systems near criticality, and is thought to be important in a wide realm of phenomena [1]. While other observations of SOC have occurred in systems which exhibit hysteretic or "avalanche" behavior [2], the self-organization reported here occurs near the continuous, nonhysteretic phase transition to superfluidity in ^{4}He [3]. We find that the self-organized state in ^{4}He facilitates a new technique for nonequilibrium measurements very close to the superfluid transition. The nature of this self-organization may be understood by employing a simple model which relates the temperature at which the system self-organizes, to the thermal conductivity of ^{4}He and the depression of the transition temperature due to a heat flux.

The study of transport properties close to a continuous phase transition is difficult because the out-of-equilibrium situation required to observe the properties generates gradients in the properties themselves. This inhomogeneous situation rounds the sharpness of the transition under study and limits the accuracy with which the measurement may be made [4]. Such problems are reduced in systems which support transport without a gradient in the associated thermodynamic potential. Examples include superfluid ^{3}He and ^{4}He, which allow heat transport without an associated temperature gradient in their superfluid phase. In the normal phase the gradient appears, making conclusive measurements of transport properties through the transition difficult. A second inhomogeneity is created by Earth's gravity which produces a static pressure gradient, and hence a gradient in the superfluid transition temperature, across the sample [5].

Onuki predicts that these two different sources of inhomogeneity can effectively offset one another, causing the helium to remain at a constant distance from criticality within its normal phase [6]. This results in a homogeneity that permits heat transport measurements much closer to criticality than is otherwise possible in the presence of temperature and pressure gradients. This is one specific example of self-organization, which is possible in systems with a divergent thermal diffusivity, as discussed by Carlson *et al.* [7]. Machta *et al.* [8] applied this theory to ^{4}He and predicted that it should self-organize near its superfluid transition. Recently, Ahlers and Liu [9] determined the conditions which would permit the experimental observation of this self-organization.

To produce self-organization, heat is applied to the top of a vertical column of helium in order to create a temperature gradient ∇T along the same direction as the gravity-induced gradient in the sample's superfluid transition temperature ∇T_λ. ∇T_λ is a constant, equal to 1.273 μK/cm near saturated vapor pressure (SVP) [5], resulting from the pressure dependence of T_λ and the hydrostatic pressure variation along the height of the cell. The heat flow equation is $\nabla T = -Q/\kappa(Q,t)$, where $t = [T - T_c(Q,z)]/T_{\lambda 0}$ is the reduced temperature, $T_{\lambda 0} = 2.1768$ K, and T_c is the temperature at which κ appears to diverge. This equation can be integrated to produce a profile of t, a measure of the proximity to criticality, throughout the sample. In the case where the sample is being heated from the top in the range of Q we investigated, the solution for t always approaches a constant value, t_{SOC}, throughout the normal fluid part of the sample. When $\nabla t = 0$, κ is also constant, ∇T equals ∇T_λ, and the heat flow equation becomes

$$\kappa(Q, t_{\mathrm{SOC}}) = \frac{|Q|}{\nabla T_\lambda}, \tag{1}$$

where $t_{\mathrm{SOC}} = [T_{\mathrm{SOC}}(Q,z) - T_c(Q,z)]/T_{\lambda 0}$ for all z. The observed divergence of κ as t approaches zero [4] implies that larger values of Q result in a smaller t_{SOC}. Thus Eq. (1) implies a single experimental path on the Q-T plane which was calculated in Ref. [9].

The cryostat used for this study is similar to one described earlier [10]. A sample of helium is contained in a 7.4 mm tall, 2 cm diameter cylinder with 510 μm thick Vespel [11] walls and aluminum end caps (Fig. 1). The temperature at three locations in the cell is monitored with three paramagnetic salt thermometers that provide sub-nano-Kelvin resolution near T_λ [12]. These thermometers are thermally connected to the helium through 25 μm thick copper foils that penetrate the Vespel sidewall. This thickness of the sidewall probes is minimized to achieve the best spatial resolution along the height of the helium sample, while still maintaining an adequate contact area with the ^{4}He to achieve sub-nano-Kelvin thermal resolution. To minimize stray heat currents, the entire support structure provides a high degree of isolation from unwanted heat sources [13].

The bottom of the cell is connected to a separate vapor pressure (VP) chamber through a 125 μm inner-diameter stainless steel capillary. The sample pressure is regulated by maintaining the temperature of a liquid-vapor ^{4}He interface in the VP chamber slightly above T_λ. Regulating the VP chamber temperature to within 0.5 μK of its set point throughout the measurements stabilizes T_λ in the sample cell to within a nK.

The helium temperature near the top of the cell was monitored with a probe (probe 1) located 1.02 mm below the top end cap. Another pair of probes (probes 2 and 3) was placed 1.35 and 1.02 mm above the bottom end cap respectively. The thermometer resolution was about 0.27 nK in a 1 Hz measurement bandwidth. The magnitudes of small, stray heat currents in the cell and through the support structure were determined by varying the amount of heat applied to the top of the cell while observing the associated response of the thermometers with the helium maintained a μK below its superfluid transition temperature. Any response of a thermometer to this test indicated an unwanted link between the thermometer and top heater that bypassed the helium. Results from this test were used to correct the data taken throughout the critical region (much closer to T_λ) and demonstrated that variations in the stray heat currents were no more than 0.01% of the applied heat.

Two methods of thermal control were used to make the SOC measurements. Method 1 allowed the sample temperature to drift slowly upward by slightly decreasing the heat removed from the cell bottom. This way the entire sample could be brought into the SOC state. Figure 2 shows a typical drift through the transition using this technique. In the figure, it is clear that, prior to the formation of normal fluid in the cell, all three thermometers tracked each other because of the near-infinite thermal conductivity of the superfluid. The temperature in the cell at this time is indicated by *A* in Figs. 1 and 2. Normal fluid first formed at the bottom of the cell where the transition temperature was the lowest. As the temperature of the cell increased, the interface between normal and superfluid moved up the cell toward the lower sidewall probes. As the interface passed a probe, the associated thermometer became decoupled from the superfluid temperature which continued to increase. The temperatures of the probes below this interface gradually stopped changing (indicated by *B*) as the reduced temperature profile below the interface approached a constant value, consistent with the SOC condition $\nabla T = 0$ discussed above. The temperature at each thermometer remained at its respective T_{SOC} as the superfluid continued to warm.

The SOC condition was satisfied throughout the entire cell shortly after the interface had reached the cell top

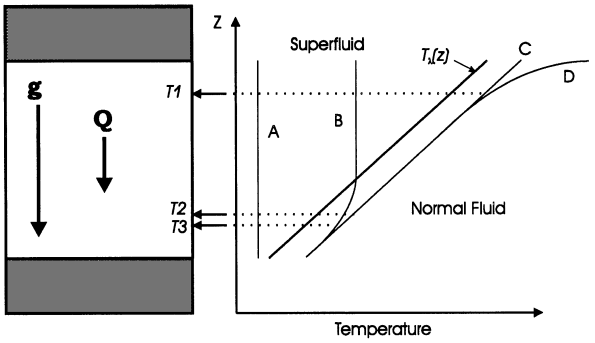

FIG. 1. A schematic of the experimental cell showing the locations of the temperature probes and the directions of gravity and the applied heat flux. Next to this is a phase diagram of temperature vs height in the cell (similar to one in Ref. [9]) with four hypothetical temperature profiles shown. Profile *A* exists when the entire cell is superfluid. Profile *B* is a typical profile that exists when the superfluid interface is between thermometers 1 and 2. Profile *C* results when the interface no longer exists in the cell and the top end plate temperature equals T_{SOC}. Profile *D* comes about when the top end plate temperature exceeds T_{SOC}.

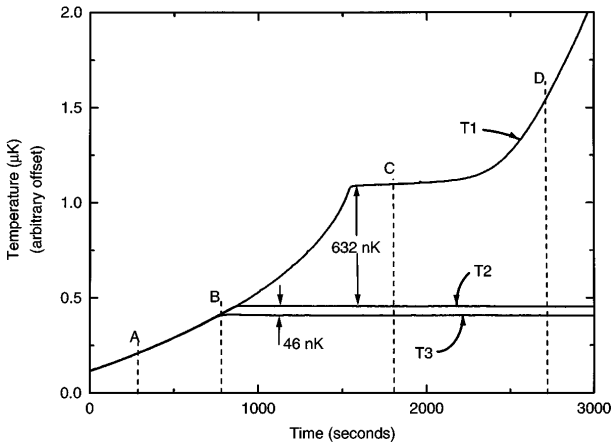

FIG. 2. Typical measurement using control method 1 at a heat flux of 482 nW/cm^2, showing the temperature profiles of each probe as the interface moves through the cell. The difference between the SOC temperatures (when the profiles become horizontal) corresponds to the physical spacing between the probes. The locations of the example profiles (A–D) from Fig. 1 are also indicated in this figure.

(indicated by C). A further increase in the cell top plate temperature pulled the helium temperature away from T_{SOC} at the top of the cell, decreasing the conductivity of the helium in this region. The point of departure from the SOC state then began to work its way down the cell as the top plate continued to warm. As this point moved downward past probe 1, T_1 again started to increase (indicated by D), causing the final upward bend in T_1 in Fig. 2. In measurements at higher values of Q, the lower part of the cell remained in the SOC state over a wide range of cell top plate temperature. Convection eventually occurred when a temperature difference of about 10 μK developed across the cell.

In the SOC state, the temperature difference between the two closely spaced probes $(T_2 - T_3)$ is 46 nK for the data shown in Fig. 2. Given a transition temperature gradient of 1.273 μK/cm [5] and the difference in probe height, the predicted temperature difference is 43 nK, which is in good agreement with the data. The temperature difference $T_1 - T_2$ in the SOC state, is 632 nK which agrees well with the predicted temperature difference of 637 nK.

The second method of thermal control (method 2) was to regulate the temperature of the superfluid in the upper region of the cell using thermometer 1 to control a heater on the bottom end cap. The temperature of the superfluid (T_1) was quasistatically ramped upward at the rate of 200 pK/s. This method required that thermometer 1 always be in contact with the superfluid. Figure 3 displayed the temperature of thermometer 2 as the interface moved past the probe. Several temperature profiles showing the approach into the SOC region for different values of Q are illustrated in Fig. 3. Notice that measurements at lower values of Q show a more gradual approach into the SOC region, indicating that the quantity $T_{\mathrm{SOC}}(Q) - T_c(Q)$ gets larger for smaller Q [9].

The solid lines in Fig. 3 display the results of a numerical solution to the heat flow equation using a simple approximation for the thermal conductivity,

$$\kappa(t) = \kappa_0 t^{-x}, \tag{2}$$

where $\kappa_0 = 12$ μW/cm K and $x = 0.44$. This approximation for $\kappa(t)$ agrees closely with thermal conductivity measurements by others [14,15] over the range $5 \times 10^{-6} < t < 10^{-4}$. The calculated thermal profiles for each Q displayed in Fig. 3 agree well with the data at low Q, but this agreement becomes systematically worse as Q increases.

Figures 4 and 5 display the results of our measurements of the SOC state temperature at probe 2 using control method 2. Since it was difficult to measure $T_{\lambda 0}$ precisely, each data point is instead referenced to a SOC state temperature at $Q_{\mathrm{ref}} = 100$ nW/cm^2. To avoid errors resulting from long term drifts of the thermometers, measurements were made at the reference heat flux every second scan. We observed that the apparent drift rate in the reference temperature was less than 10^{-13} K/s, indicating good experimental stability in temperature, pressure, and heat flux.

To develop a simple model for this data, we can replace the thermal conductivity in Eq. (1) with the approximation for κ in Eq. (2) to obtain an equation for t_{SOC},

$$t_{\mathrm{SOC}}(Q) = \left(\frac{\kappa_0 \nabla T_\lambda}{|Q|}\right)^{1/x}. \tag{3}$$

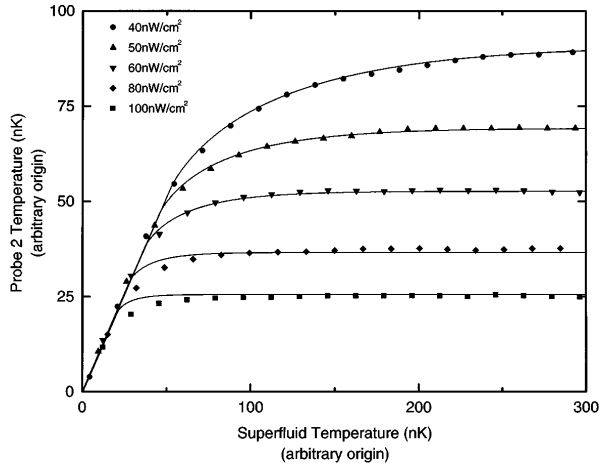

FIG. 3. sidewall probe temperature T_2 vs the superfluid temperature T_1 for the different values of Q shown in the inset. This figure shows how T_2 approaches its local T_{SOC} after the interface passes the probe. The solid lines display numerical solutions to the heat flow equation that use the approximate form of thermal conductivity discussed in the text. Each numerical curve is given a single constant offset to fit the data on the right side of the figure in the SOC region.

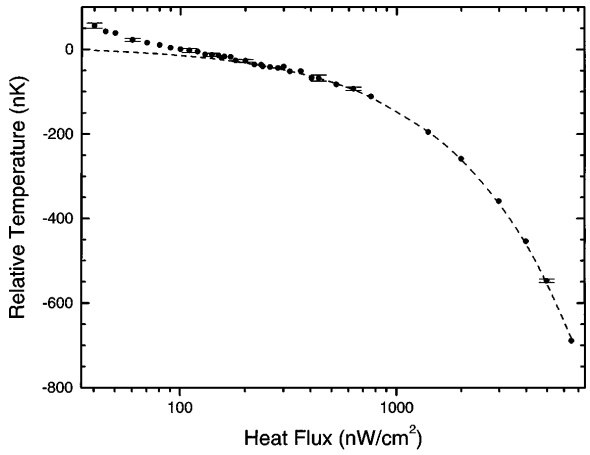

FIG. 4. SOC temperature data taken with probe 2 over the entire range of Q used in this study. Each data point is referenced to the SOC temperature at $Q_{\mathrm{ref}} = 100$ nW/cm^2. The dashed curve is a calculation of $T_c(Q) - T_{\mathrm{SOC}}(Q_{\mathrm{ref}})$ using Eqs. (6) and (4), respectively. As expected, the data follows the numerical prediction for $T_c(Q)$ closely only for higher values of Q.

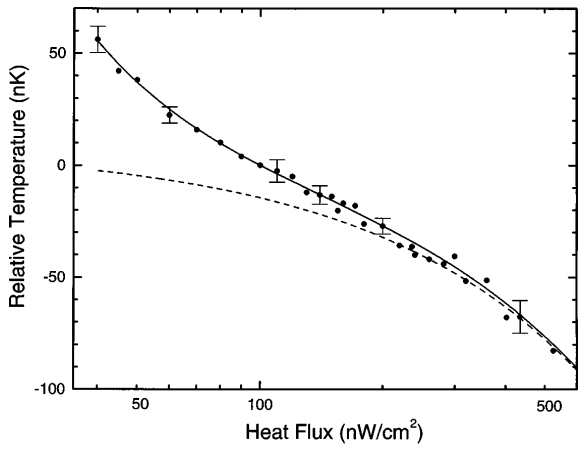

FIG. 5. Low heat flux data replotted from Fig. 4. The dashed curve is the same curve as the one in Fig. 4. The solid curve is a fit to the data using Eq. (4) for $T_{\mathrm{SOC}}(Q)$, Eq. (6) for $T_c(Q)$, and Eq. (5) for $\Delta T_{\mathrm{SOC}}(Q)$.

Inserting the definition of the reduced temperature into Eq. (3), an expression for the SOC state temperature T_{SOC} becomes

$$T_{\mathrm{SOC}}(Q) = T_c(Q) + \Delta T_{\mathrm{SOC}}(Q), \tag{4}$$

where

$$\Delta T_{\mathrm{SOC}} = T_{\lambda 0}\left(\frac{\kappa_0 \nabla T_\lambda}{|Q|}\right)^{1/x} \tag{5}$$

is the difference between $T_{\mathrm{SOC}}(Q)$ and $T_c(Q)$. For $Q > 500$ nW/cm^2, $\Delta T_{\mathrm{SOC}}(Q)$ becomes less than the thermometer resolution so that, in this range of heat flux, $T_{\mathrm{SOC}}(Q) \approx T_c(Q)$.

Data taken by other authors [16] for $T_c(Q)$ in the range $0.45 \leq Q \leq 10$ μW/cm^2 suggest the depression of T_c with Q can be represented by an equation of the form,

$$T_c(Q) = T_{\lambda 0}\left(1 - \left|\frac{Q}{Q_0}\right|^y\right). \tag{6}$$

A fit of our data over the range $Q > 500$ nW/cm^2 to the equation $T_c(Q) - T_{\mathrm{SOC}}(Q_{\mathrm{ref}})$ gives values of $Q_0 = 638 \pm 178$ W/cm^2 and $y = 0.813 \pm 0.012$. This fit is in good agreement with Ref. [16] and is plotted along with our data in Figs. 4 and 5 as a dashed line. At lower values of Q, where ΔT_{SOC} is no longer negligible, a more direct knowledge of $\kappa(t)$ is required to extract $T_c(Q)$ from the data.

Figure 5 shows how the data for the range $Q < 500$ nW/cm^2 depart from the calculated $T_c(Q) - T_{\mathrm{SOC}}(Q_{\mathrm{ref}})$ which is indicated by the dashed line in the figure. For this range of Q, $T_{\mathrm{SOC}}(Q)$ can no longer be approximated by $T_c(Q)$, but must now include the term $\Delta T_{\mathrm{SOC}}(Q)$ which may be estimated using Eq. (5). The solid curve plotted in Fig. 5 is a fit of Eqs. (4) and (5) to our data. This fit gives values of $\kappa_0 = 294 \pm 89$ nW/cm K, and $x = 0.664 \pm 0.016$.

In conclusion, we have observed the predicted self-organization of the thermal conductivity of ^{4}He near its superfluid transition by applying heat to the top of a sample of helium. The SOC state temperature was measured for a range of heat flux $0.40 \leq Q \leq 6.5$ μW/cm^2. For values of $Q > 500$ nW/cm^2, the SOC temperature is a direct measurement of $T_c(Q)$ and agrees closely with previous data for $T_c(Q)$. Measurements in the low-Q limit where $T_c(Q) \approx T_{\lambda 0}$, should provide an accurate means of determining $\kappa(Q, t_{\mathrm{SOC}})$ once the low-Q variation of $T_c(Q)$ has been determined experimentally.

We gratefully acknowledge the assistance of Kim Aaron, Yuri Mukharsky, Al Nash, and Chris Paine with the construction of the apparatus. We also thank Richard Ferrell and Guenter Ahlers for discussions which motivated this work. This research has been sponsored by the Microgravity Science and Applications Division of NASA under Contract No. 957448, and by the Department of Energy under Contract No. DE-AC04-94AL85000.

[1] Per Bak, *How Nature Works* (Copernicus, Springer-Verlag, New York, 1996).
[2] P. Bak, C. Tang, and K. Wiesenfeld, Phys. Rev. A **38**, 364 (1988).
[3] F. C. Liu and Guenter Ahlers, Physica (Amsterdam) **194B-196B**, 597 (1994).
[4] See, for instance, Guenter Ahlers and Robert Duncan, in *Frontiers of Physics*, edited by E. Gotsman, Y. Ne'eman, and A. Voronel, Proceedings of the Landau Memorial Conference (Pergamon Press, New York, 1990), p. 219.
[5] G. Ahlers, Phys. Rev. **171**, 275 (1968).
[6] A. Onuki, Jpn. J. Appl. Phys. **26**, 365 (1987); J. Low Temp. Phys. **104**, 133 (1996).
[7] J. M. Carlson, J. T. Chayes, E. R. Grannan, and G. H. Swindle, Phys. Rev. Lett. **65**, 2547 (1990).
[8] J. Machta, D. Candela, and R. B. Hallock, Phys. Rev. B **47**, 4581 (1993).
[9] G. Ahlers and F-C. Liu, J. Low Temp. Phys. **105**, 255 (1996).
[10] M. J. Adriaans, W. A. Moeur, S. T. P. Boyd, D. M. Strayer, and R. V. Duncan, Cryogenics **36**, 787 (1996).
[11] F. Pobell, *Matter and Methods at Low Temperatures* (Springer-Verlag, New York, 1992), p. 60.
[12] J. A. Lipa, B. C. Leslie, and T. C. Wallstrom, Physica (Amsterdam) **107B**, 331 (1981).
[13] A. E. Nash, *et al.*, Proceedings of the 35th Aerospace Sciences Meeting, AIAA 97-0782, Reno, Nevada, 1997 (to be published).
[14] W. Y. Tam and G. Ahlers, Phys. Rev. B **32**, 5932 (1985); **33**, 183 (1986).
[15] M. Dingus, F. Zhong, and H. Meyer, J. Low Temp. Phys. **65**, 185 (1986).
[16] R. V. Duncan, G. Ahlers, and V. Steinberg, Phys. Rev. Lett. **60**, 1522 (1988).